mathematics

MDPI

Article

Quasi-Periodic Oscillations of Roll System in Corrugated Rolling Mill in Resonance

Dongping He [1,2], Huidong Xu [1,2,*], Tao Wang [1,2] and Zhihua Wang [1,2]

[1] College of Mechanical and Vehicle Engineering, Taiyuan University of Technology, Taiyuan 030024, China; hedongping@tyut.edu.cn (D.H.); wangtao01@tyut.edu.cn (T.W.); wangzhihua@tyut.edu.cn (Z.W.)
[2] Institute of Advanced Forming and Intelligent Equipment, Taiyuan University of Technology, Taiyuan 030024, China
* Correspondence: xuhuidong@tyut.edu.cn

Abstract: This paper investigates quasi-periodic oscillations of roll system in corrugated rolling mill in resonance. The two-degree of freedom vertical nonlinear mathematical model of roller system is established by considering the nonlinear damping and nonlinear stiffness within corrugated interface of corrugated rolling mill. In order to investigate the quasi-periodic oscillations at the resonance points, the Poincaré map is established by solving the power series solution of dynamic equations. Based on the Poincaré map, the existence and stability of quasi-periodic oscillations from the Neimark-Sacker bifurcation in the case of resonance are analyzed. The numerical simulation further verifies the correctness of the theoretical analysis.

Keywords: corrugated rolling mill; resonance; quasi-periodic oscillation; Poincaré map; Neimark-Sacker bifurcation

check for updates

Citation: He, D.; Xu, H.; Wang, T.; Wang, Z. Quasi-Periodic Oscillations of Roll System in Corrugated Rolling Mill in Resonance. *Mathematics* **2021**, *9*, 3201. https://doi.org/10.3390/math9243201

Academic Editors: Youming Lei and Lijun Pei

Received: 12 November 2021
Accepted: 8 December 2021
Published: 11 December 2021

1. Introduction

The corrugated rolling mill is a multivariable, strongly coupled, multi-constrained and time-varying non-linear system. The phenomena of resonance may occur during the rolling process of composite plates due to the sinusoidal roll profile curve of the corrugated roller and the nonlinear damping and stiffness between corrugated roll and flat roll. The resonance will cause the fluctuation of roll gap and further affect the bonding strength of the composite plates and reduce the online service time of rolls. It is of great theoretical and practical significance to research the vibration behavior of rolling mill in resonance.

Over the past several decades, many researchers have investigated the vibration and the bifurcation phenomena of rolling mill. However, there are many factors affecting rolling mill vibration, which is a crossing research topic of vibration theory, rolling theory and bifurcation control. Therefore, it is still challenging for the research of the vibration of the rolling mill. Johnson and Qi [1] analyzed the influence of the nonlinearity of contact interface between the work roll and the supporting roll on the rolling mill dynamics and found that the nonlinearity could cause high frequency harmonic vibration. Swiatoniowski [2] investigated the dynamic behavior of vertical vibration of rolling system by considering the elastoplastic deformation as nonlinear elastic force. Yarita et al. [3] proposed a two-degree-of-freedom vertical vibration system and studied the parameter excited resonance by analyzed the fluctuating variation of stiffness between rollers. Kapil et al. [4] developed a nonlinear parameter excited vibration single-degree of freedom model of the rolling mill and obtained the amplitude-frequency vibration characteristics and unstable region of the rolling mill. Li and Wen [5] established a nonlinear vibration mechanical model by considering the clearance and vibration boundary of the main drive system of the rolling mill and investigated various dynamic responses such as periodic, quasi-periodic and chaotic vibrations. Huang and Zang [6] established the dynamic equation of the main drive system of the rolling mill by considering nonlinear friction resistance and obtained the necessary and sufficient conditions of Hopf bifurcation in the system. Hou et al. [7,8] established the torsional vibration equation of the main drive system of the rolling mill by considering the nonlinear factors, such as piecewise nonlinearity, clearance, and nonlinear friction damping of the roll system, and investigated a variety of dynamic behaviors of the system. Liu et al. [9,10] studied the sliding bifurcation of a horizontal-torsional coupled main drive system of rolling mill and Hopf bifurcation control of a coupled nonlinear relative rotation system with time-delay feedbacks. Aiming at the difficulty to establish accurate traditional mechanism model for cold rolling vibration, Zhou et al. [11] established the gradient boosted decision tree model to perform vibration energy regression by using production data measured on site. Qian et al. [12] established the 4 DOF mechanical hydraulic coupling model based on the analysis of the coupling effect of rolling mill hydraulic and mechanical systems. Qi et al. [13] investigated the influence of the mill modulus control gain on the vibration in hot rolling mills through experiments and numerical simulations.

Neimark-Sacker bifurcation is a second Hopf bifurcation of the original system. The typical solution of Neimark-Sacker bifurcation is the quasi-periodic torus solution. Many researchers pay attention to the Neimark-Sacker bifurcation of various mechanical systems in non-resonant case. Chatterjee and Mallik [14] investigated the quasi-periodic vibro-impact behaviors of a class of self-excited oscillators. Budd et al. [15] considered a vibro-impact oscillator with a single stop to analyze the effect of frequency and clearance variations on the system and proved that the quasi-periodic motion cannot occur in such systems. Cui et al. [16] studied the existence of quasi-periodic solutions of the Van der pol-Duffing oscillator by HAM method. Wen et al. [17] addressed the anti-controlling quasi-periodic impact motion of an inertial impact shaker system by developing a linear feedback control method. However, there are few studies on Neimark-Sacker bifurcation at the resonance point of a mechanical system. Guo and Xie [18] investigated Neimark-Sacker Bifurcation of an oscillator with dry friction in 1:4 strong resonance. To the authors' best knowledge, there is no literature focused on studying quasi-periodic oscillations from Neimark-Sacker bifurcation at the resonance point for roll system of corrugated rolling mill.

The main purpose of the present paper is to investigate the quasi-periodic oscillations from the Neimark-Sacker bifurcation in resonance for the roll system of the corrugated rolling mill. In Section 2, the two-degree of freedom nonlinear vertical vibration mathematical model is established by considering the nonlinear damping and stiffness within corrugated interface of corrugated rolling mill. The Poincaré map is derived by solving the power series solution of dynamic equations in Section 3. Based on the Poincaré map, the existence of the Neimark-Sacker bifurcation and the stability of quasi-periodic oscillations in strong resonance and weak resonance are analyzed, and theoretical analysis is verified by the numerical simulation in Section 4. A conclusion is drawn in Section 5.

2. The Mechanical Model and Dynamic Equation of Corrugated Rolling Mill

The roller system of a corrugated rolling mill with the nonlinear damping and nonlinear stiffness within the corrugated interface of a corrugated rolling mill can be simplified into a two-freedom-degree vertical nonlinear vibration model, as is shown in Figure 1. The m_1 and m_2 represent the equivalent mass of the corrugated roll and the equivalent mass of the flat roll, respectively; k_1 and c_1 are the stiffness and the average damping value between the corrugated roll and rack, respectively; k_2 and c_2 are the stiffness and the average damping value between the flat roll and rack, respectively, and k_0 and c_0 are the average value of stiffness and the average value of damping in steady state of corrugated rolling mill, respectively. $F_0\ \sin \omega t$ is approximately the rolling force during the rolling process. The F_0 is rolling the force amplitude, and ω is the rolling force frequency. The damping between the corrugated roll and flat roll caused by the roll shape curve is defined as $c_0 + c'_0(y_1 - y_2)^2$. The c'_0 represents the nonlinear damping coefficient of roller systems. The stiffness between the roller system and rack is defined as $k_i + k'_i y_i^2$ $(i = 1, 2)$. The k'_i represents the nonlinear stiffness coefficient of roller systems. The initial position for system (1) is set to the zero position.

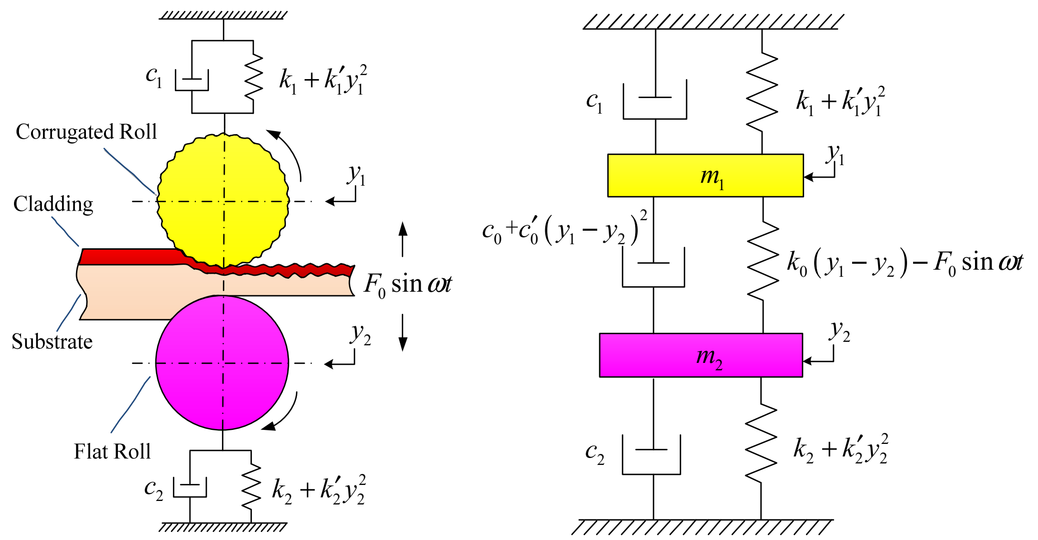

Figure 1. The rolling diagram of corrugated rolling mill: (**left**) the mechanical model; (**right**) two-freedom-degree vertical nonlinear vibration model.

The nonlinear parameter excited vibration equations of the roller system can be established as follows:

$$\begin{cases} m_1\ddot{y}_1(t) + \left(c_0 + c'_0(y_1(t) - y_2(t))^2\right)(\dot{y}_1(t) - \dot{y}_2(t)) + c_1\dot{y}_1(t) + (k_1 + k'_1 y_1^2(t))y_1(t) \\ +k_0(y_1(t) - y_2(t)) - F_0 \sin\omega t = 0 \\ m_2\ddot{y}_2(t) - \left(c_0 + c'_0(y_1(t) - y_2(t))^2\right)(\dot{y}_1(t) - \dot{y}_2(t)) + c_2\dot{y}_2(t) + (k_2 + k'_2 y_2^2(t))y_2(t) \\ -k_0(y_1(t) - y_2(t)) + F_0 \sin\omega t = 0 \end{cases} \tag{1}$$

As the roller system has approximate symmetry, we suppose that $m_1 = m_2$ and $y_1(t) = -y_2(t)$. Thus, system (1) can be simplified as follows:

$$m_1\ddot{y}_1(t) + \left(2c_0 + c_1 + 2c'_0(2y_1(t))^2\right)\dot{y}_1(t) + \left(k_1 + k'_1 y_1^2(t)\right)y_1(t) + 2k_0 y_1(t) - F_0 \sin\omega t = 0 \tag{2}$$

If $\omega_0^2 = \frac{2k_0+k_1}{m_1}$, $\alpha = \frac{2c_0+c_1}{m_1}$, $\beta = \frac{8c'_0}{m_1}$, $\gamma = \frac{k'}{m_1}$, $F = \frac{F_0}{m_1}$, and $\theta = \omega t$, system (2) can be written as follows:

$$\ddot{y}_1(t) + {\omega_0}^2 y_1(t) + \left(\alpha + \beta {y_1}^2(t)\right)\dot{y}_1(t) + \gamma y_1^3(t) - F\sin(\theta) = 0 \tag{3}$$

Using the transformation $\begin{bmatrix} y_1(t) \\ \dot{y}_1(t) \end{bmatrix} = \begin{bmatrix} 1 & 0 \\ 0 & -\omega_0 \end{bmatrix}\begin{bmatrix} x_1(t) \\ x_2(t) \end{bmatrix}$, system (3) is transformed into the following standard form:

$$\begin{cases} \dot{x}_1(t) = -\omega_0 x_2(t) \\ \dot{x}_2(t) = \omega_0 x_1(t) - (\alpha + \beta x_1^2(t))x_2(t) + \frac{\gamma}{\omega_0} x_1^3(t) - \frac{F}{\omega_0}\sin(\theta) \end{cases} \tag{4}$$

3. The Poincaré Map

When the quasi-periodic oscillations of the system (4) in resonance is studied, the derivative of θ with respect to time t is $\dot{\theta} = n\omega_0 (n = 3, 4, 5)$. Through introducing the new time τ and scaling the original time by $t = \tau/\omega_0$, system (5) with respect to τ are given by

$$\begin{cases} \frac{dx_1(\tau)}{d\tau} = -x_2(\tau) \\ \frac{dx_2(\tau)}{d\tau} = x_1(\tau) - \frac{1}{\omega_0}\big(\alpha + \beta x_1^2(\tau)\big)x_2(\tau) + \frac{1}{\omega_0^2}\gamma x_1^3(\tau) - \frac{1}{\omega_0^2}F\sin(\theta) \\ \frac{d\theta}{d\tau} = n \end{cases} \tag{5}$$

Suppose that $-\frac{\alpha}{\omega_0} = \mu$, $-\frac{\beta}{\omega_0} = a$, $\frac{\gamma}{\omega_0^2} = b$, $-\frac{F}{\omega_0^2} = \varepsilon$, system (5) can be written as follows:

$$\begin{cases} \dot{x}_1(\tau) = -x_2(\tau) \\ \dot{x}_2(\tau) = x_1(\tau) + \mu x_2(\tau) + a x_1^2(\tau)x_2(\tau) + b x_1^3(\tau) + \varepsilon\sin(\theta) \\ \dot{\theta} = n \end{cases} \tag{6}$$

where the dot (.) denotes the derivative with respect to τ.

In order to establish Poincaré map, let $z(\tau) = x_1(\tau) + ix_2(\tau)$, and then, let system (6) be changed into

$$\dot{z}(\tau) = iz(\tau) + \mu\frac{z(\tau) - \bar{z}(\tau)}{2} + a\left(\frac{z(\tau) + \bar{z}(\tau)}{2}\right)^2\frac{(z(\tau) - \bar{z}(\tau))}{2} + ib\left(\frac{z(\tau) + \bar{z}(\tau)}{2}\right)^3 + i\varepsilon\sin(\theta) \tag{7}$$

According to continuous dependence on the parameters of the solution, the solution to system (7) is expanded as a Taylor series in the parameters μ and ε as:

$$\begin{aligned} z(\eta, \tau, \mu, \varepsilon) = \quad & z_0(\eta, \tau) + \mu z_{10}(\eta, \tau) + \varepsilon z_{01}(\eta, \tau) + \\ & \mu\varepsilon z_{11}(\eta, \tau) + \tfrac{1}{2}\mu^2 z_{20}(\eta, \tau) + \tfrac{1}{2}\varepsilon^2 z_{02}(\eta, \tau) + \cdots \end{aligned} \tag{8}$$

which satisfies the initial value condition $z(\eta, 0, \mu, \varepsilon) = \eta$.

Substituting solution (8) into system (7) and collecting coefficients of primary and quadratic terms of μ and ε, we can obtain

$$\dot{z}_0(\eta, \tau) = iz_0(\eta, \tau) + \frac{a}{8}(z_0 + \bar{z}_0)^2(z_0 - \bar{z}_0) + \frac{ib}{8}(z_0 + \bar{z}_0)^3 \tag{9}$$

$$\begin{aligned} \dot{z}_{10}(\eta, \tau) = \quad & iz_{10}(\eta, \tau) + \tfrac{(z_0 - \bar{z}_0)}{2} + \tfrac{a}{4}(z_0 + \bar{z}_0)(z_0 - \bar{z}_0)(z_{10} + \bar{z}_{10}) \\ & + \tfrac{a}{8}(z_0 + \bar{z}_0)^2(z_{10} - \bar{z}_{10}) + \tfrac{3ib}{8}(z_0 + \bar{z}_0)^2(z_{10} + \bar{z}_{10}) \end{aligned} \tag{10}$$

$$\begin{aligned} \dot{z}_{01}(\eta, \tau) = \quad & iz_{01}(\eta, \tau) + \tfrac{a}{4}(z_0 + \bar{z}_0)(z_0 - \bar{z}_0)(z_{01} + \bar{z}_{01}) \\ & + \tfrac{a}{8}(z_0 + \bar{z}_0)^2(z_{01} - \bar{z}_{01}) + \tfrac{3ib}{8}(z_0 + \bar{z}_0)^2(z_{01} + \bar{z}_{01}) + i\sin(\theta) \end{aligned} \tag{11}$$

$$\begin{aligned} \dot{z}_{11}(\eta, \tau) = \quad & iz_{11}(\eta, \tau) + \tfrac{(z_{01} - \bar{z}_{01})}{2} + \tfrac{a}{4}(z_{01} + \bar{z}_{01})(z_0 - \bar{z}_0)(z_{10} + \bar{z}_{10}) \\ & + \tfrac{a}{4}(z_0 + \bar{z}_0)(z_{01} - \bar{z}_{01})(z_{10} + \bar{z}_{10}) + \tfrac{a}{4}(z_0 + \bar{z}_0)(z_0 - \bar{z}_0)(z_{11} + \bar{z}_{11}) \\ & + \tfrac{a}{4}(z_0 + \bar{z}_0)(z_{10} - \bar{z}_{10})(z_{01} + \bar{z}_{01}) + \tfrac{a}{8}(z_0 + \bar{z}_0)^2(z_{11} - \bar{z}_{11}) \\ & + \tfrac{6ib}{8}(z_0 + \bar{z}_0)(z_{10} + \bar{z}_{10})(z_{01} + \bar{z}_{01}) + \tfrac{3ib}{8}(z_0 + \bar{z}_0)^2(z_{11} + \bar{z}_{11}) \end{aligned} \tag{12}$$

$$\begin{aligned} \dot{z}_{20}(\eta, \tau) = \quad & \tfrac{i}{2}z_{20}(\eta, \tau) + \tfrac{1}{2}(z_{10} - \bar{z}_{10}) + \tfrac{a}{8}(z_{10} + \bar{z}_{10})^2(z_0 - \bar{z}_0) + \\ & + \tfrac{a}{4}(z_0 + \bar{z}_0)(z_{10} - \bar{z}_{10})(z_{10} + \bar{z}_{10}) + \tfrac{a}{8}(z_0 + \bar{z}_0)(z_0 - \bar{z}_0)(z_{20} + \bar{z}_{20}) \\ & + \tfrac{a}{16}(z_0 + \bar{z}_0)^2(z_{20} - \bar{z}_{20}) + \tfrac{3ib}{8}(z_0 + \bar{z}_0)(z_{10} + \bar{z}_{10})^2 \\ & + \tfrac{3ib}{16}(z_0 + \bar{z}_0)^2(z_{20} + \bar{z}_{20}) \end{aligned} \tag{13}$$

$$\begin{aligned}\dot{z}_{02}(\eta,\tau) = \; & \tfrac{i}{2}z_{02}(\eta,\tau) + \tfrac{a}{8}(z_{01}+\overline{z}_{01})^2(z_0-\overline{z}_0) + \tfrac{a}{4}(z_0+\overline{z}_0)(z_{01}-\overline{z}_{01})(z_{01}+\overline{z}_{01}) \\ & + \tfrac{a}{8}(z_0+\overline{z}_0)(z_0-\overline{z}_0)(z_{02}+\overline{z}_{02}) + \tfrac{a}{16}(z_0+\overline{z}_0)^2(z_{02}-\overline{z}_{02}) \\ & + \tfrac{3ib}{8}(z_0+\overline{z}_0)(z_{01}+\overline{z}_{01})^2 + \tfrac{3ib}{16}(z_0+\overline{z}_0)^2(z_{02}+\overline{z}_{02})\end{aligned} \tag{14}$$

The solutions $z_0(\eta,\tau)$, $z_{10}(\eta,\tau)$, $z_{01}(\eta,\tau)$, $z_{11}(\eta,\tau)$, $z_{20}(\eta,\tau)$, and $z_{02}(\eta,\tau)$ of Equations (10)–(15) are also expanded as Taylor series in the initial values η and $\overline{\eta}$ as:

$$\begin{aligned}z_0(\eta,\tau) = \; & L_{10}\eta + L_{01}\overline{\eta} + \tfrac{L_{20}}{2}\eta^2 + L_{11}\eta\overline{\eta} + \tfrac{L_{02}}{2}\overline{\eta}^2 + \tfrac{L_{30}}{6}\eta^3 + \tfrac{L_{21}}{2}\eta^2\overline{\eta} + \tfrac{L_{12}}{2}\eta\overline{\eta}^2 \\ & + \tfrac{L_{03}}{6}\overline{\eta}^3 + \tfrac{L_{40}}{24}\eta^4 + \tfrac{L_{31}}{6}\eta^3\overline{\eta} + \tfrac{L_{22}}{4}\eta^2\overline{\eta}^2 + \tfrac{L_{13}}{6}\eta\overline{\eta}^3 + \tfrac{L_{04}}{24}\overline{\eta}^4 + (\ldots)\end{aligned} \tag{15}$$

$$z_{10}(\eta,\tau) = A_{10}\eta + A_{01}\overline{\eta} + (\ldots) \tag{16}$$

$$z_{01}(\eta,\tau) = B_{00} + B_{10}\eta + B_{01}\overline{\eta} + (\ldots) \tag{17}$$

$$z_{11}(\eta,\tau) = C_{00} + C_{10}\eta + C_{01}\overline{\eta} + (\ldots) \tag{18}$$

$$z_{20}(\eta,\tau) = D_{10}\eta + D_{01}\overline{\eta} + (\ldots) \tag{19}$$

$$z_{02}(\eta,\tau) = E_{10}\eta + E_{01}\overline{\eta} + (\ldots) \tag{20}$$

where L_{ij}, A_{ij}, B_{ij}, C_{ij}, D_{ij} and E_{ij} are the abbreviations for $L_{ij}(\tau)$, $A_{ij}(\tau)$, $B_{ij}(\tau)$, $C_{ij}(\tau)$, $D_{ij}(\tau)$, and $E_{ij}(\tau)$, respectively.

As the cases of 1:3, 1:4 and 1:5 resonances are analyzed in the system, it is enough that $z_0(\eta,\tau)$ is expanded to fourth order terms of the initial value. Since $z_{10}(\eta,\tau)$, $z_{01}(\eta,\tau)$, $z_{11}(\eta,\tau)$, $z_{20}(\eta,\tau)$, and $z_{02}(\eta,\tau)$ are multiplied by small parameters, it is enough that their series solutions are expanded to first order terms. Substituting Solution (15) into Equation (9) and collecting coefficients of corresponding terms of η and $\overline{\eta}$, we have

$$\dot{L}_{10} = iL_{10},\ \dot{L}_{01} = iL_{01},\ \dot{L}_{20} = iL_{20},\ \dot{L}_{11} = iL_{11},\ \dot{L}_{02} = iL_{02},$$

$$\dot{L}_{30} = iL_{30} + \frac{3ib-3\mathrm{a}}{4}\overline{L}_{01}^3 + \frac{9ib-3\mathrm{a}}{4}L_{10}\overline{L}_{01}^2 + \frac{9ib+3\mathrm{a}}{4}L_{10}^2\overline{L}_{01} + \frac{3ib+3\mathrm{a}}{4}L_{10}^3$$

$$\begin{aligned}\dot{L}_{21} = \; & iL_{21} + \tfrac{3ib-3\mathrm{a}}{4}\overline{L}_{01}^2\overline{L}_{10} + \tfrac{3ib-\mathrm{a}}{4}\overline{L}_{01}^2L_{01} + \tfrac{3ib-\mathrm{a}}{2}L_{10}\overline{L}_{01}\overline{L}_{10} \\ & + \tfrac{3ib+\mathrm{a}}{2}L_{10}\overline{L}_{01}L_{01} + \tfrac{3ib+\mathrm{a}}{4}L_{10}^2\overline{L}_{10} + \tfrac{3ib+3\mathrm{a}}{4}L_{10}^2L_{01}\end{aligned}$$

$$\begin{aligned}\dot{L}_{12} = \; & iL_{12} + \tfrac{3ib-3\mathrm{a}}{4}\overline{L}_{10}^2\overline{L}_{01} + \tfrac{3ib-\mathrm{a}}{4}\overline{L}_{10}^2L_{10} + \tfrac{3ib-\mathrm{a}}{2}L_{01}\overline{L}_{10}\overline{L}_{01} \\ & + \tfrac{3ib+\mathrm{a}}{2}L_{01}\overline{L}_{10}L_{10} + \tfrac{3ib+\mathrm{a}}{4}L_{01}^2\overline{L}_{01} + \tfrac{3ib+3\mathrm{a}}{4}L_{01}^2L_{10}\end{aligned}$$

$$\dot{L}_{03} = iL_{03} + \frac{3ib-3\mathrm{a}}{4}\overline{L}_{10}^3 + \frac{9ib-3\mathrm{a}}{4}L_{01}\overline{L}_{10}^2 + \frac{9ib+3\mathrm{a}}{4}L_{01}^2\overline{L}_{10} + \frac{3ib+3\mathrm{a}}{4}L_{01}^3$$

$$\begin{aligned}\dot{L}_{40} = \; & iL_{40} + \tfrac{9ib-9\mathrm{a}}{2}\overline{L}_{01}^2\overline{L}_{02} + \tfrac{9ib-3\mathrm{a}}{2}\overline{L}_{01}^2L_{20} + (9ib-3\mathrm{a})\overline{L}_{02}L_{10}\overline{L}_{01} \\ & + (9ib+3\mathrm{a})L_{20}L_{10}\overline{L}_{01} + \tfrac{9ib+3\mathrm{a}}{2}L_{10}^2\overline{L}_{02} + \tfrac{9ib+9\mathrm{a}}{2}L_{10}^2L_{20}\end{aligned}$$

$$\begin{aligned}\dot{L}_{31} = \; & iL_{31} + \tfrac{9ib-9\mathrm{a}}{4}\overline{L}_{01}^2\overline{L}_{11} + \tfrac{9ib-3\mathrm{a}}{4}\overline{L}_{01}^2L_{11} + \tfrac{9ib-3\mathrm{a}}{2}\overline{L}_{11}L_{10}\overline{L}_{01} \\ & + \tfrac{9ib+3\mathrm{a}}{2}L_{11}L_{10}\overline{L}_{01} + \tfrac{9ib-9\mathrm{a}}{4}\overline{L}_{10}\overline{L}_{02}\overline{L}_{01} + \tfrac{9ib-9\mathrm{a}}{4}L_{01}\overline{L}_{02}\overline{L}_{01} \\ & + \tfrac{9ib-3\mathrm{a}}{4}\overline{L}_{10}L_{20}\overline{L}_{01} + \tfrac{9ib+3\mathrm{a}}{4}L_{01}L_{20}\overline{L}_{01} + \tfrac{9ib+3\mathrm{a}}{4}L_{10}^2\overline{L}_{11} + \tfrac{9ib+9\mathrm{a}}{4}L_{10}^2L_{11} \\ & + \tfrac{9ib-3\mathrm{a}}{4}\overline{L}_{10}\overline{L}_{02}L_{10} + \tfrac{9ib+3\mathrm{a}}{4}L_{01}\overline{L}_{02}L_{10} + \tfrac{9ib+3\mathrm{a}}{4}\overline{L}_{10}L_{20}L_{10} + \tfrac{9ib+9\mathrm{a}}{4}L_{01}L_{20}L_{10}\end{aligned}$$

$$\begin{aligned}
\dot{L}_{22} = \; & iL_{22} + \tfrac{3(ib-\mathrm{a})}{4}\overline{L}_{01}^{2}\overline{L}_{20} + \tfrac{3ib-\mathrm{a}}{4}\overline{L}_{01}^{2}L_{02} + (3ib-3\mathrm{a})\overline{L}_{11}\overline{L}_{10}\overline{L}_{01} + (3ib-\mathrm{a})L_{11}\overline{L}_{10}\overline{L}_{01} \\
& + \tfrac{3ib-\mathrm{a}}{2}\overline{L}_{20}L_{10}\overline{L}_{01} + \tfrac{3ib+\mathrm{a}}{2}L_{02}L_{10}\overline{L}_{01} + (3ib-\mathrm{a})\overline{L}_{11}L_{01}\overline{L}_{01} + (3ib+\mathrm{a})L_{11}L_{01}\overline{L}_{01} \\
& + \tfrac{3(ib-\mathrm{a})}{4}\overline{L}_{10}^{2}\overline{L}_{02} + \tfrac{3ib-\mathrm{a}}{4}\overline{L}_{10}^{2}L_{20} + (3ib-\mathrm{a})\overline{L}_{11}L_{10}\overline{L}_{10} + (3ib+\mathrm{a})L_{11}L_{10}\overline{L}_{10} \\
& + \tfrac{3ib-\mathrm{a}}{2}\overline{L}_{02}L_{01}\overline{L}_{10} + \tfrac{3ib+\mathrm{a}}{2}L_{20}L_{01}\overline{L}_{10} + \tfrac{3ib+\mathrm{a}}{4}L_{10}^{2}\overline{L}_{20} + \tfrac{3ib+3\mathrm{a}}{4}L_{10}^{2}L_{02} \\
& + (3ib+\mathrm{a})\overline{L}_{11}L_{01}L_{10} + (3ib+3\mathrm{a})L_{11}L_{01}L_{10} + \tfrac{3ib+\mathrm{a}}{4}L_{01}^{2}\overline{L}_{02} + \tfrac{3ib+3\mathrm{a}}{4}L_{01}^{2}L_{20}
\end{aligned}$$

$$\begin{aligned}
\dot{L}_{13} = \; & iL_{13} + \tfrac{9ib-9\mathrm{a}}{4}\overline{L}_{10}^{2}\overline{L}_{11} + \tfrac{9ib-3\mathrm{a}}{4}\overline{L}_{10}^{2}L_{11} + \tfrac{9ib-3\mathrm{a}}{2}\overline{L}_{11}L_{01}\overline{L}_{10} \\
& + \tfrac{9ib+3\mathrm{a}}{2}L_{11}L_{01}\overline{L}_{10} + \tfrac{9ib-9\mathrm{a}}{4}\overline{L}_{01}\overline{L}_{20}\overline{L}_{10} + \tfrac{9ib-3\mathrm{a}}{4}L_{10}\overline{L}_{20}\overline{L}_{10} \\
& + \tfrac{9ib-3\mathrm{a}}{4}\overline{L}_{01}L_{02}\overline{L}_{10} + \tfrac{9ib+3\mathrm{a}}{4}L_{10}L_{02}\overline{L}_{10} + \tfrac{9ib+3\mathrm{a}}{4}L_{01}^{2}\overline{L}_{11} + \tfrac{9ib+9\mathrm{a}}{4}L_{01}^{2}L_{11} \\
& \tfrac{9ib-3\mathrm{a}}{4}\overline{L}_{01}\overline{L}_{20}L_{01} + \tfrac{9ib+3\mathrm{a}}{4}L_{10}\overline{L}_{20}L_{01} + \tfrac{9ib+3\mathrm{a}}{4}\overline{L}_{01}L_{02}L_{01} + \tfrac{9ib+9\mathrm{a}}{4}L_{10}L_{02}L_{01}
\end{aligned}$$

$$\begin{aligned}
\dot{L}_{04} = \; & iL_{04} + \tfrac{9ib-9\mathrm{a}}{2}\overline{L}_{10}^{2}\overline{L}_{20} + \tfrac{9ib-3\mathrm{a}}{2}\overline{L}_{10}^{2}L_{02} + (9ib-3\mathrm{a})\overline{L}_{20}L_{01}\overline{L}_{10} \\
& + (9ib+3\mathrm{a})L_{02}L_{01}\overline{L}_{10} + \tfrac{9ib+3\mathrm{a}}{2}L_{01}^{2}\overline{L}_{20} + \tfrac{9ib+9\mathrm{a}}{2}L_{01}^{2}L_{02}
\end{aligned}$$

which satisfies the initial value condition as:

$$L_{10}(0) = 1,\; L_{01}(0) = 1,\; L_{20}(0) = 1,\; L_{11}(0) = 1,\; L_{02}(0) = 1,$$

$$L_{30}(0) = 0,\; L_{21}(0) = 0,\; L_{12}(0) = 0,\; L_{03}(0) = 0,$$

$$L_{40}(0) = 0,\; L_{31}(0) = 0,\; L_{22}(0) = 0,\; L_{13}(0) = 0,\; L_{04}(0) = 0.$$

Through solving the differential equations on $L_{ij}(\tau)$, we obtain

$$L_{10}(\tau) = L_{01}(\tau) = e^{i\tau},\; L_{20}(\tau) = L_{02}(\tau) = e^{i\tau},\; L_{11}(\tau) = e^{i\tau},$$

$$\begin{aligned}
L_{30}(\tau) = \; & ((0.94i + 0.75\tau)a + (0.94 + 2.25i\tau)b)e^{i\tau} - 0.19(b + ai)e^{-3i\tau} \\
& -(1.13b + 0.38ai)e^{-i\tau} + 0.38(b - ai)e^{3i\tau}
\end{aligned}$$

$$L_{03}(\tau) = L_{21}(\tau) = L_{12}(\tau) = L_{30}(\tau),$$

$$\begin{aligned}
L_{40}(\tau) = \; & ((5.63i + 4.5\tau)a + (5.63 + 13.5i\tau)b)e^{i\tau} - 1.13(b + ai)e^{-3i\tau} \\
& -(6.75b + 2.25ai)e^{-i\tau} + 2.25(b - ai)e^{3i\tau}
\end{aligned}$$

$$L_{04}(\tau) = L_{31}(\tau) = L_{13}(\tau) = L_{22}(\tau) = L_{40}(\tau).$$

Letting $\sin(\theta)= \sin(n\tau)$ $(n = 3,\ 4,\ 5)$ and substituting the above series solution of $z_0(\eta,\tau)$ in Equations (10)–(14), the coefficients of series solutions on $z_{10}(\eta,\tau)$, $z_{01}(\eta,\tau)$, $z_{11}(\eta,\tau)$, $z_{20}(\eta,\tau)$ and $z_{02}(\eta,\tau)$ are obtained as:

$$A_{10} = A_{01} = \frac{2\tau + i}{4}e^{i\tau} - \frac{i}{4}e^{-i\tau}$$

$$B_{00} = e^{-\int -id\tau}\int i\sin(n\tau)e^{\int -id\tau}d\tau + Ce^{-\int -id\tau}(n = 3,\ 4,\ 5)\ , B_{00}(0) = 0$$

$$B_{10} = B_{01} = e^{i\tau},$$

$$C_{00} = e^{-\int -id\tau}\int \frac{B_{00} - \overline{B}_{00}}{2}e^{\int -id\tau}d\tau + Ce^{-\int -id\tau}(n = 3,\ 4,\ 5), C_{00}(0) = 0$$

$$C_{10} = C_{01} = \frac{2\tau + i}{4}e^{i\tau} - \frac{i}{4}e^{-i\tau}$$

$$D_{10} = D_{01} = \frac{2\tau^2 - 1 + 2\tau i}{8}e^{i\tau} + \frac{1}{8}e^{-i\tau}$$

$$E_{10} = e^{-\int -id\tau}\int Q_{10}e^{\int -id\tau}d\tau + Ce^{-\int -id\tau}(n = 3,\ 4,\ 5),\ E_{10}(0) = 0$$

$$\begin{aligned} Q_{10} = \ & \overline{B}_{00}^2\left[\tfrac{3(ib-a)}{4}\overline{L}_{10} + \tfrac{3ib-a}{4}L_{10}\right] + \left(\tfrac{3ib-a}{2}\overline{L}_{10} + \tfrac{3ib+a}{2}L_{10}\right)B_{00}\overline{B}_{00} \\ & + B_{00}^2\left[\tfrac{3ib+a}{4}\overline{L}_{10} + \tfrac{3(ib+a)}{4}L_{10}\right] \end{aligned}$$

$$E_{01} = e^{-\int -id\tau}\int Q_{01}e^{\int -id\tau}d\tau + Ce^{-\int -id\tau}(n=3,\ 4,\ 5),\ E_{01}(0)=0$$

$$\begin{aligned} Q_{01} = \ & \overline{B}_{00}^2\left[\tfrac{3(ib-a)}{4}\overline{L}_{01} + \tfrac{3ib-a}{4}L_{01}\right] + \left(\tfrac{3ib-a}{2}\overline{L}_{01} + \tfrac{3ib+a}{2}L_{01}\right)B_{00}\overline{B}_{00} \\ & + B_{00}^2\left(\tfrac{3ib+a}{4}\overline{L}_{01} + \tfrac{3(ib+a)}{4}L_{01}\right) \end{aligned}$$

Substituting the above results of L_{ij}, A_{ij}, B_{ij}, C_{ij}, D_{ij}, and E_{ij} into the solution (8), we obtain the series solution to Equation (7). Based on the series solution, when the Poincaré section is chosen as $\tau = \frac{2\pi}{n}(n=3,\ 4,\ 5)$, the Poincaré map in the case of resonance can be presented as:

$$\begin{aligned} \eta \mapsto z\left(\eta, \tfrac{2\pi}{n}, \mu, \varepsilon\right) = \ & z_0\left(\eta, \tfrac{2\pi}{n}\right) + \mu z_{10}\left(\eta, \tfrac{2\pi}{n}\right) + \varepsilon z_{01}\left(\eta, \tfrac{2\pi}{n}\right) + \mu\varepsilon z_{11}\left(\eta, \tfrac{2\pi}{n}\right) \\ & + \tfrac{1}{2}\mu^2 z_{20}\left(\eta, \tfrac{2\pi}{n}\right) + \tfrac{1}{2}\varepsilon^2 z_{02}\left(\eta, \tfrac{2\pi}{n}\right) + \ldots \\ & = e^{i\frac{2\pi}{n}}(\eta+\overline{\eta}) + \mu\left(\tfrac{4\pi+in}{4n}e^{i\frac{2\pi}{n}} - \tfrac{i}{4}e^{-i\frac{2\pi}{n}}\right)(\eta+\overline{\eta}) + \varepsilon e^{i\frac{2\pi}{n}}(\eta+\overline{\eta}) \\ & + \varepsilon B_{00} + \mu\varepsilon C_{00} + \mu\varepsilon\left(\tfrac{4\pi+in}{4n}e^{i\frac{2\pi}{n}} - \tfrac{i}{4}e^{-i\frac{2\pi}{n}}\right)(\eta+\overline{\eta}) + \tfrac{g_{20}}{2}\eta^2 \\ & + \tfrac{1}{2}\mu^2\left(\tfrac{8\pi^2+4\pi ni-n^2}{8n^2}e^{i\frac{2\pi}{n}} + \tfrac{1}{8}e^{-i\frac{2\pi}{n}}\right)(\eta+\overline{\eta}) + \tfrac{1}{2}\varepsilon^2(E_{10}\eta + E_{01}\overline{\eta}) \\ & + \tfrac{1}{2}\varepsilon^2(E_{10}\eta + E_{01}\overline{\eta}) + g_{11}\eta\overline{\eta} + \tfrac{g_{02}}{2}\overline{\eta}^2 + \tfrac{g_{30}}{6}\eta^3 + \tfrac{g_{21}}{2}\eta^2\overline{\eta} + \tfrac{g_{12}}{2}\eta\overline{\eta}^2 \\ & + \tfrac{g_{03}}{6}\overline{\eta}^3 + \tfrac{g_{40}}{24}\eta^4 + \tfrac{g_{31}}{6}\eta^3\overline{\eta} + \tfrac{g_{22}}{4}\eta^2\overline{\eta}^2 + \tfrac{g_{13}}{6}\eta\overline{\eta}^3 + \tfrac{g_{04}}{24}\overline{\eta}^4 + o(\ldots) \end{aligned} \tag{21}$$

Due to $G(\eta,\ \mu,\ \varepsilon) = \left[z\left(\eta, \frac{2\pi}{n}, \mu, \varepsilon\right) - \eta\right]\Big|_{\eta=0,\ \mu=0,\ \varepsilon=0} = 0$ and $\frac{\partial}{\partial\eta}G(\eta,\ \mu,\ \varepsilon)\Big|_{\eta=0,\ \mu=0,\ \varepsilon=0} = e^{i\tau} - 1 \neq 0 \ \left(\tau = \frac{2\pi}{n}(n=3,\ 4,\ 5)\right)$, the map (21) has a fixed point as denoted by η^*, which continuously depends on parameters μ and ε according to the implicit function theorem.

Theorem 1. *By solving the power series solution of dynamic equations and using the transformation of coordinate $\xi = \eta - \eta^*$, the Poincaré map for system (6) is established as follows:*

$$\begin{aligned} \xi \mapsto \Psi(\xi, \mu, \varepsilon) \ & = e^{i\frac{2\pi}{n}}(\xi+\overline{\xi}) + \mu\left(\tfrac{4\pi+in}{4n}e^{i\frac{2\pi}{n}} - \tfrac{i}{4}e^{-i\frac{2\pi}{n}}\right)(\xi+\overline{\xi}) + \varepsilon e^{i\frac{2\pi}{n}}(\xi+\overline{\xi}) \\ & + \mu\varepsilon\left(\tfrac{4\pi+in}{4n}e^{i\frac{2\pi}{n}} - \tfrac{i}{4}e^{-i\frac{2\pi}{n}}\right)(\xi+\overline{\xi}) + \tfrac{1}{2}\varepsilon^2(E_{10}\xi + E_{01}\overline{\xi}) + \tfrac{g_{20}}{2}\xi^2 + g_{11}\xi\overline{\xi} \\ & + \tfrac{1}{2}\mu^2\left(\tfrac{8\pi^2+4\pi ni-n^2}{8n^2}e^{i\frac{2\pi}{n}} + \tfrac{1}{8}e^{-i\frac{2\pi}{n}}\right)(\xi+\overline{\xi}) + \tfrac{g_{02}}{2}\overline{\xi}^2 + \tfrac{g_{30}}{6}\xi^3 + \tfrac{g_{21}}{2}\xi^2\overline{\xi} \\ & + \tfrac{g_{12}}{2}\xi\overline{\xi}^2 + \tfrac{g_{03}}{6}\overline{\xi}^3 + \tfrac{g_{40}}{24}\xi^4 + \tfrac{g_{31}}{6}\xi^3\overline{\xi} + \tfrac{g_{22}}{4}\xi^2\overline{\xi}^2 + \tfrac{g_{13}}{6}\xi\overline{\xi}^3 + \tfrac{g_{04}}{24}\overline{\xi}^4 + o(\ldots) \end{aligned} \tag{22}$$

where, $g_{20} = L_{20}$, $g_{11} = L_{11}$, $g_{02} = L_{02}$, $g_{30} = L_{30}$, $g_{21} = L_{21}$, $g_{12} = L_{12}$, $g_{03} = L_{03}$, $g_{40} = L_{40}$, $g_{31} = L_{31}$, $g_{22} = L_{22}$, $g_{13} = L_{13}$, $g_{04} = L_{04}$.

It follows from the map (22) that the eigenvalue has the following form:

$$\begin{aligned} \lambda(\mu, \varepsilon) = \ & e^{i\frac{2\pi}{n}}\Big(1 + \left(\tfrac{4\pi+in}{4n} - \tfrac{i}{4}e^{-i\frac{4\pi}{n}}\right)\mu + \varepsilon + \left(\tfrac{4\pi+in}{4n} - \tfrac{i}{4}e^{-i\frac{4\pi}{n}}\right)\mu\varepsilon \\ & + \left(\tfrac{8\pi^2+4\pi ni-n^2}{16n^2} + \tfrac{1}{16}e^{-i\frac{4\pi}{n}}\right)\mu^2 + \tfrac{1}{2}E_{10}e^{-i\frac{2\pi}{n}}\varepsilon^2 + o(\ldots)\Big) \end{aligned} \tag{23}$$

The eigenvalue (23) can be simplified as

$$\lambda(\mu, \varepsilon) = e^{i\frac{2\pi}{n}}\left(1 + \widetilde{\lambda}\mu + o(\ldots)\right), \quad \left(\widetilde{\lambda} = \left(\frac{4\pi+in}{4n} - \frac{i}{4}e^{-i\frac{4\pi}{n}}\right)\right) \tag{24}$$

4. Neimark-Sacker Bifurcation in Resonance

4.1. 1:3 Resonance

When Neimark-Sacker bifurcation in 1:3 strong resonance occurs in the roll system, through using the appropriate transformation and letting $\sin(\theta) = \sin(3\tau)$ $(n = 3)$, the map (22) can be transformed into the normal form as [19]:

$$\zeta \mapsto \Phi_1(\zeta,\ \mu) = \lambda\zeta + \gamma\overline{\zeta}^2 + \alpha\zeta^2\overline{\zeta} + O\left(|\zeta|^5\right) \tag{25}$$

Through calculation, some coefficients at $\mu = 0$ of map (25) can be obtained as:

$$\lambda(0) = -\frac{1}{2} + \frac{\sqrt{3}}{2}i,\ \gamma(0) = \frac{g_{02}(0)}{2} = -\frac{1}{4} + \frac{\sqrt{3}}{4}i,$$

$$\begin{aligned} \alpha(0) &= \tfrac{2\lambda(0)-1}{2\lambda(0)(1-\lambda(0))}g_{11}(0)g_{20}(0) + \tfrac{|g_{11}(0)|^2}{1-\overline{\lambda}(0)} + \tfrac{g_{21}(0)}{2} \\ &= 0.75 - 1.01i + (-0.96 + 0.26i)a - (1.9 + 0.29i)b \end{aligned} \tag{26}$$

Lemma 1. *[20] If* $\frac{\partial}{\partial\mu}|\lambda(\mu)|\Big|_{\mu=0} = \mathrm{Re}\left(\widetilde{\lambda}\right) > 0$, *a stable invariant cycle (corresponding to a stable quasi-periodic oscillation of the original roll system) can appear through a Neimark-Sacker bifurcation when* $\mu > 0$ *if* $\mathrm{Re}(\alpha(0)/\lambda(0)) < 0$, *and an unstable invariant cycle arises in the system when* $\mu < 0$ *if* $\mathrm{Re}(\alpha(0)/\lambda(0)) > 0$.

When the parameters $\varepsilon = -0.1$, $a = -1.5$, $b = 0.6$ are taken as an example and substituted into the expressions (24) and (26), we have $\frac{\partial}{\partial\mu}|\lambda(\mu)|\Big|_{\mu=0} = 1.26 > 0$ and $\mathrm{Re}(\alpha(0)/\lambda(0)) = -1.88 < 0$. This means that the map (25) has a stable fixed point when $\mu < 0$, as is shown in the left-hand sketch of Figure 2, which corresponds to a stable periodic oscillation of the original roll system (6) as shown in the right-hand sketch of Figure 2. When $\mu > 0$, the fixed point loses its stability, and a stable invariant cycle appears through Neimark-Sacker bifurcation, as is shown in the left-hand sketch of Figure 3, which corresponds to a stable quasi-periodic oscillation of the original roll system (6) as shown in the right-hand sketch of Figure 3.

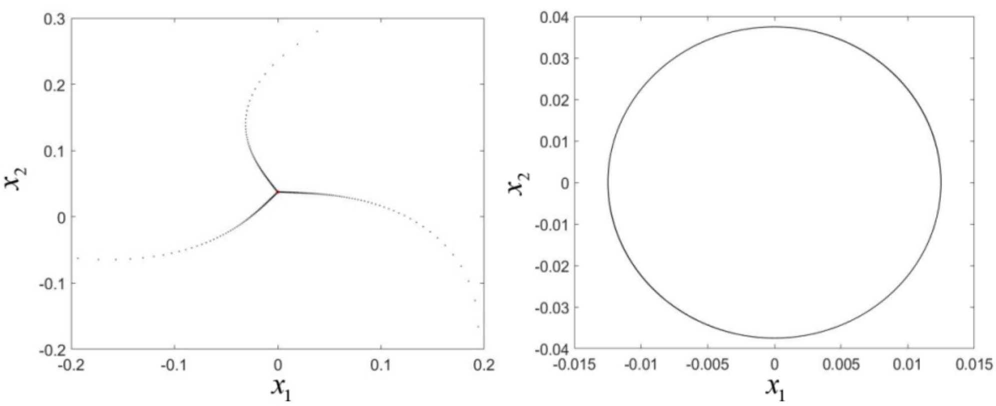

Figure 2. The stable periodic motion in 1:3 resonance when $\mu = -0.01$: (**left**) the stable fixed point; (**right**) the stable periodic motion.

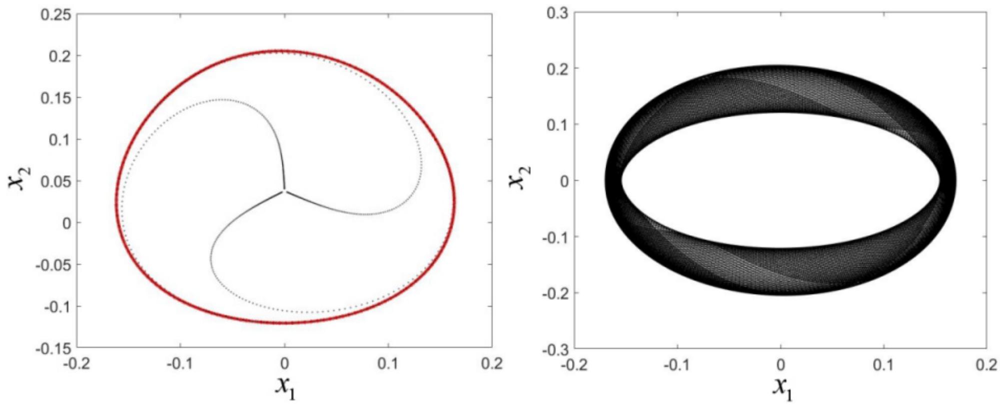

Figure 3. The stable quasi-periodic motion in 1:3 resonance when $\mu = 0.01$: (**left**) the stable invariant circle; (**right**) the stable quasi-periodic motion.

4.2. 1:4 Resonance

Using the appropriate transformation, the map (22) in 1:4 resonance can be transformed into the normal form as [19]:

$$\zeta \mapsto \Phi_2(\zeta,\ \mu) = \lambda\zeta + \sigma\zeta^2\overline{\zeta} + \beta\overline{\zeta}^3 + O\left(|\zeta|^5\right) \tag{27}$$

Some coefficients at $\mu = 0$ of map (27) are calculated as:

$$\begin{aligned} \lambda(0) = i, \quad \sigma\,(0) &= \frac{g_{21}(0)}{2} + \frac{|g_{11}(0)|^2}{1-\overline{\lambda}(0)} + \frac{|g_{02}(0)|^2}{2\left(\lambda^2(0)-\overline{\lambda}(0)\right)} + \frac{2\lambda(0)-1}{2\lambda(0)(1-\lambda(0))}g_{11}(0)g_{20}(0) \\ &= (-0.75+0.59i)a + (-1.77+0.75i)b - 1.5i \\ \beta(0) &= \frac{1}{2\lambda(0)(\lambda(0)-1)}g_{11}(0)g_{02}(0) + \frac{g_{02}(0)g_{20}(0)}{2\left(\lambda^2(0)-\overline{\lambda}(0)\right)} + \frac{g_{03}(0)}{6} \\ &= (-0.25+0.2i)a + (-0.59+0.25i)b - 0.5i \end{aligned} \tag{28}$$

Lemma 2. *[20] If $\left|\mathrm{Im}\left(\frac{\sigma}{\lambda}\right)\right| > \left|\frac{\beta}{\lambda}\right|$, there is no period 4 orbit bifurcating from the fixed point of map (27). The stable invariant circle can bifurcate from the fixed point when $\mathrm{Re}(\alpha(0)/\lambda(0)) < 0$. The unstable invariant circle can bifurcate from the fixed point when $\mathrm{Re}(\alpha(0)/\lambda(0)) > 0$.*

Lemma 3. *[20] If $\left|\mathrm{Im}\left(\frac{\sigma}{\lambda}\right)\right| < \left|\frac{\beta}{\lambda}\right|$, the period 4 orbits can bifurcate from the fixed point of map (27). Furthermore, if $|\sigma| > |\beta|$, the period 4 orbits exist on one side of the critical value of parameter, and at least one of them is unstable. If $|\sigma| < |\beta|$, the period 4 orbits exist on both sides of the critical parameter, all of which are unstable.*

Choosing $\varepsilon = -0.15$, $a = -5.5$, $b = 0.1$ and according to the expressions (24) and (28), we obtain $\left|\mathrm{Im}\left(\frac{\sigma}{\lambda}\right)\right| - \left|\frac{\beta}{\lambda}\right| = 4.32 > 0$ and $\mathrm{Re}(\alpha(0)/\lambda(0)) = -4.66 < 0$. Based on Lemma 2, we assert that the map (27) has a stable invariant circle. According to the expression (23), we can calculate that $\frac{\partial}{\partial\mu}|\lambda(\mu)|\Big|_{\mu=0} = 0.79 > 0$. This means a stable fixed point as shown in the left-hand sketch of Figure 4 exists in the map (27) when $\mu < 0$, which corresponds to the stable periodic motion of the original system, as is shown in the right-hand sketch of Figure 4. When $\mu > 0$, there exists a stable invariant circle as shown in the left-hand sketch of Figure 5 bifurcating from the fixed point, which corresponds to the stable quasi-periodic motion of the original system, as is shown in the right-hand sketch of Figure 5.

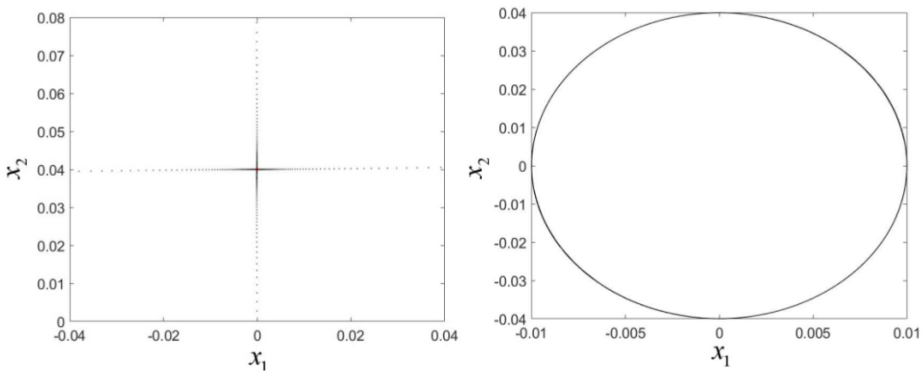

Figure 4. The stable periodic motion in 1:4 resonance when $\mu = -0.02$: (**left**) the stable fixed point; (**right**) the stable periodic motion.

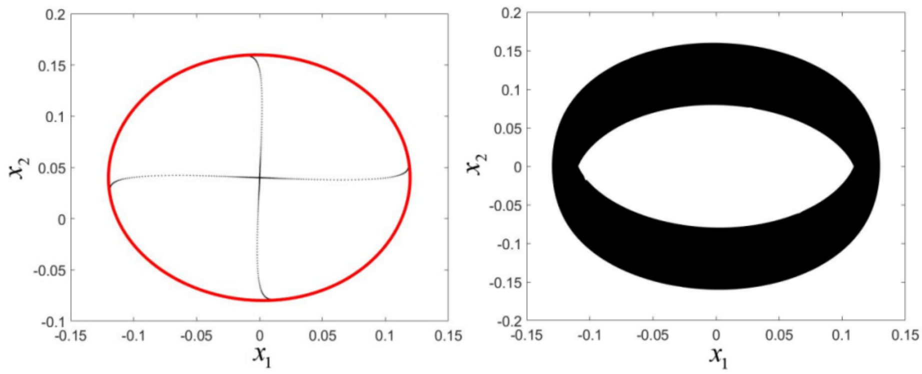

Figure 5. The stable quasi-periodic motion in 1:4 resonance when $\mu = 0.02$: (**left**) the stable invariant circle; (**right**) the stable quasi-periodic motion.

4.3. 1:5 Resonance

Using the appropriate transformation, the map (22) in 1:5 resonance can be transformed into the normal form as [19]:

$$\zeta \mapsto \Phi_3(\zeta,\ \mu) = \lambda\zeta + \delta\zeta^2\bar{\zeta} + O\left(|\zeta|^5\right) \tag{29}$$

Some coefficients at $\mu = 0$ of map (29) are calculated as:

$$\lambda(0) = \cos\left(\frac{2\pi}{5}\right) + i\sin\left(\frac{2\pi}{5}\right)$$

$$\begin{aligned}\delta(0) &= \tfrac{2\lambda(0)-1}{2\lambda(0)(1-\lambda(0))} g_{11}(0)g_{20}(0) + \tfrac{|g_{11}(0)|^2}{1-\bar{\lambda}(0)} + \tfrac{g_{21}(0)}{2} \\ &= -0.06 - 1.29i + (-0.53 + 0.76i)a + (-1.45 + 1.25i)b\end{aligned}$$

Lemma 4. *[20] If* $\mathrm{Re}(\alpha(0)/\lambda(0)) < 0$*, the stable invariant circle can bifurcate from the fixed point of map (29). The unstable invariant circle can bifurcate from the fixed point for* $\mathrm{Re}(\alpha(0)/\lambda(0)) > 0$.

The parameters $\varepsilon = -0.1$, $a = -2.5$ and $b = 0.8$ are chosen as an example. It follows from the expressions (30) and (23) that $\mathrm{Re}(\alpha(0)/\lambda(0)) = -2.06 < 0$ and $\frac{\partial}{\partial\mu}|\lambda(\mu)|\Big|_{\mu=0} = 0.48 > 0$ are obtained. Based on Lemma 4, the map (29) has a stable fixed point as shown in the left-hand sketch of Figure 6 when $\mu < 0$, which corresponds to the stable periodic motion of the original system, as is shown in the right-hand sketch of Figure 6. There exists a stable invariant circle, as shown in the left-hand sketch of Figure 7, bifurcating from the fixed point when $\mu > 0$, which corresponds to the stable quasi-periodic motion of the original system, as is shown in the right-hand sketch of Figure 7.

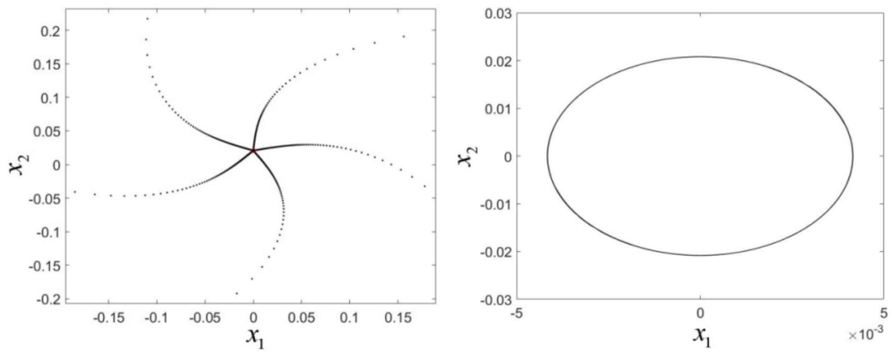

Figure 6. The stable periodic motion in 1:5 resonance when $\mu = -0.01$: (**left**) the stable fixed point; (**right**) the stable periodic motion.

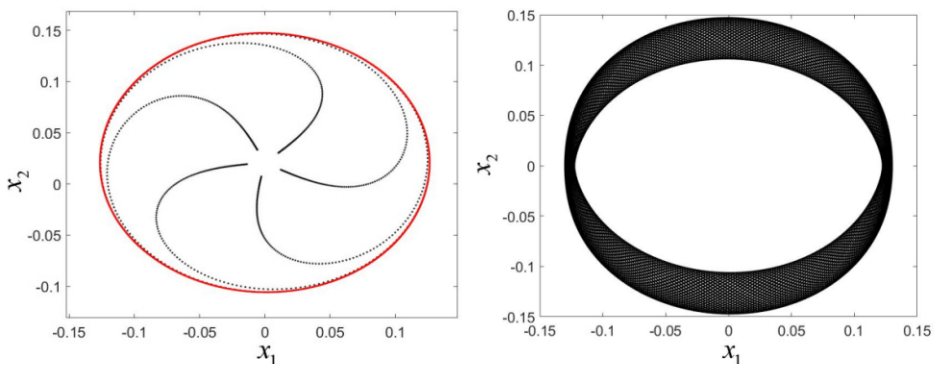

Figure 7. The stable quasi-periodic motion in 1:5 resonance when $\mu = 0.01$: (**left**) the stable invariant circle; (**right**) the stable quasi-periodic motion.

5. Conclusions

The quasi-periodic oscillations in 1:3, 1:4 and 1:5 resonances have been studied in the roll system of a corrugated rolling mill. The Poincaré map has been established through deriving the series solution of vibration equations. The existence and stability of quasi-periodic oscillations from the Neimark-Sacker bifurcation in resonance have been analyzed. The numerical simulations have been carried out to show the stable quasi-periodic oscillations in the roll system and validate the feasibility of the theoretical method. The results can provide some useful information for structural optimizing design of the roller system of the corrugated rolling mill.

Author Contributions: Writing—original draft preparation, D.H.; writing—review and editing H.X.; funding acquisition, T.W.; supervision, Z.W. All authors have read and agreed to the published version of the manuscript.

Funding: This research was funded by National Key Research and Development Project, grant number 2018YFA0707300 and TW was also funded by National Natural Science Foundation of China, grant number 51974196.

Institutional Review Board Statement: Not applicable.

Informed Consent Statement: Not applicable.

Data Availability Statement: The datasets generated and analyzed during the current study are available from the corresponding author on reasonable request.

Acknowledgments: The authors would like to acknowledge support from the Engineering Research Center of Advanced Metal Composites Forming Technology and Equipment, Ministry of Education.

Conflicts of Interest: The authors declare no conflict of interest.

References

1. Johnson, R.E.; Qi, Q. Chatter dynamics in sheet rolling. *Int. J. Mech. Sci.* **1994**, *36*, 617–630. [CrossRef]
2. Swiatoniowski, A. Interdependence between rolling mill vibrations and the plastic deformation process. *J. Mater. Process. Technol.* **1996**, *61*, 354–364. [CrossRef]
3. Yarita, I.; Furukawa, K.; Seino, Y. Analysis of chattering in cold rolling for ultrathin gauge steel strip. *Trans. Iron Steel Inst. Jpn.* **1978**, *18*, 1–10. [CrossRef]
4. Kapil, S.; Eberhard, P.; Dwivedy, S.K. Nonlinear dynamic analysis of a parametrically excited cold rolling mill. *J. Manuf. Sci. Eng.* **2014**, *136*, 041012. [CrossRef]
5. Li, H.G.; Wen, B.C. Nonlinear vibrations of self-excited vibration systems with clearances and oscillating boundaries. *J. Vib. Eng.* **2000**, *13*, 122–127.
6. Huang, H.D.; Zang, Y. Analysis nonlinear friction caused of self-excited vibration of main drive system on rolling mill. *Coal Technol.* **2012**, *31*, 222–224.
7. Hou, D.X.; Liu, B.; Shi, P.M.; Liu, S. Bifurcation of piecewise nonlinear roll system of rolling mill. *J. Vib. Shock* **2010**, *29*, 132–135.
8. Hou, D.X.; Liu, B.; Shi, P.M.; Liu, F.; Liu, Y.J. Vibration characteristics of 2 DOF nonlinear torsional vibration system of rolling mill and its conditions of instability. *J. Vib. Shock* **2012**, *31*, 32–36.
9. Liu, S.; Li, X.; Li, Y.Q.; Li, H.B. Stability and bifurcation for a coupled nonlinear relative rotation system with multi-time delay feedbacks. *Nonlinear Dyn.* **2014**, *77*, 923–934. [CrossRef]
10. Liu, S.; Wang, Z.L.; Wang, J.J.; Li, H.B. Sliding bifurcation research of a horizontal–torsional coupled main drive system of rolling mill. *Nonlinear Dyn.* **2016**, *83*, 441–455. [CrossRef]
11. Zhou, X.M.; Hao, Y.K.; Cong, W.T.; Wei, Z.B.; Wen, G.D. Flutter analysis of cold tandem rolling mills based on gradient boosted decision tree. *J. Vib. Shock* **2021**, *40*, 154–158.
12. Qian, C.; Sun, R.S.; Zhang, L.L.; Bai, Z.H.; Hua, C.C. Coupled vibration model and influencing factors analysis of tandem cold rolling mill. *J. Mech. Eng.* **2021**, *57*, 208–216.
13. Qi, J.B.; Wang, X.X.; Yan, X.Q. Influence of mill modulus control gain on vibration in hot rolling mills. *J. Iron Steel Res Int.* **2020**, *27*, 528–536. [CrossRef]
14. Chatterjee, S.; Mallik, A.K. Bifurcations and chaos in autonomous self-excited oscillators with impact damping. *J. Sound Vib.* **1996**, *191*, 539–562. [CrossRef]
15. Budd, C.; Dux, F.; Cliffe, A. The effect of frequency and clearance variations on single-degreeof-freedom impact oscillators. *J. Sound Vib.* **1995**, *184*, 475–502. [CrossRef]
16. Cui, J.F.; Zhang, W.Y.; Liu, Z. On the limit cycles, period-doubling, and quasi-periodic solutions of the forced Van der Pol-Duffing oscillator. *Numer. Algorithms* **2018**, *78*, 1217–1231. [CrossRef]
17. Wen, G.; Xu, H.; Chen, Z. Anti-controlling quasi-periodic impact motion of an inertial impact shaker system. *J. Sound Vib.* **2010**, *329*, 4040–4047. [CrossRef]
18. Guo, Y.; Xie, J.H. N-S Bifurcation of an oscillator with dry friction in 1:4 strong resonance. *Appl. Math. Mech. Engl.* **2013**, *34*, 27–36. [CrossRef]
19. Kuznetsov, Y.A. *Element of Applied Bifurcation Theory*, 2nd ed.; Springer: New York, NY, USA, 1998.
20. Iooss, G. *Bifurcation of Maps and Applications*; Mathematical Studies, 36; North-Holland: Amsterdam, The Netherlands, 1979.